Sputtering of hollow atoms from carbon surfaces

T. Schlathölter,[1,*] A. Närmann,[1] A. Robin,[2] D. F. A. Winters,[1] S. Marini,[1] R. Morgenstern,[1] and R. Hoekstra[1]
[1]*KVI Atomic Physics, Rijksuniversiteit Groningen, 9747 AA Groningen, The Netherlands*
[2]*Universität Osnabrück, Fachbereich Physik, 49069 Osnabrück, Germany*
(Received 19 June 2000; published 13 September 2000)

We investigated the emission of *K* Auger electrons from collisions of hydrogenlike ions C^{5+}, N^{6+}, and O^{7+} with graphite as well as fullerene covered gold surfaces. Besides the quite well understood Auger electrons emitted from the projectile, an extremely high yield of Auger electrons originating from surface atoms is observed. Remarkably the target Auger spectra show discrete (atomic) *KLL* lines superimposed on the broad *KVV* spectra originating from bulk carbon. This indicates high-sputtering yields of highly excited carbon ions/atoms with *K*-shell vacancies.

PACS number(s): 34.50.Dy, 34.70.+e, 79.20.Rf

I. INTRODUCTION

The interaction of highly charged ions with solids depends strongly on the electronic properties of the surface (for a review, see Ref. [1]). For instance, very recently we could show that in particular the target work function influences the formation of a hollow atom above the surface and its subsequent deexcitation dynamics [2]. Carbon surfaces are an ideal target to study the interplay between the surface electronic properties and the neutralization dynamics of a slow ($v \ll 1$ a.u.) highly charged ion: Different allotropes can be investigated, such as graphite (sp^2 bond), diamond (sp^3 bond), and fullerenes (sp^2 and sp^3 bonds) as bulk or thin film. The electronic properties of these carbon allotropes vary between semimetallic and insulating. In this paper, we focus on Auger electrons emitted during collisions of hydrogenlike ions with carbon surfaces. Auger emission [3–9] as well as x-ray emission [10–12] from the projectile have been the subject of several studies, but emission from the target itself has been reported only for a number of collision systems.

In several early experiments, the appearance of carbon *K* Auger electrons indicated the presence of contaminants such as hydrocarbons on the surface [13–16]. In later studies focussing on the formation and deexcitation of target *K*-shell vacancies, different mechanisms inducing the vacancy formation were invoked. Schippers *et al.* [4] explained the target Auger emission induced by hydrogenlike nitrogen, oxygen, and neon in terms of a Landau-Zener-like vacancy exchange mechanism. Very fast neutralization of Ar^{q+} ions scattered from highly oriented pyrolytic graphite (HOPG) was observed by Winecki *et al.* [17]. This could not be understood by gentle overbarrier capture [18–20] of target valence electrons into high-*n* projectile states alone. Additional side feeding of the Ar *M* shell from the target *K* and *L* shell had to be invoked, implying the formation of target *K*-shell vacancies. Above the surface, side feeding could be described by the over-barrier model [18], whereas for close collisions below the surface, e.g., the molecular-orbital model by Stolterfoht *et al.* [9] has been applied. In a recent study on collisions of hydrogenlike Ar with SiO_2, Lehnert *et al.* [21] observed radiative deexcitation of Si *K*-shell vacancies, which they attributed to x-ray fluorescence induced by photons from radiative projectile deexcitation. A similar scheme based on Auger electrons could be imagined. Common to all these studies is the fact, that only emission from target atoms embedded in the surface or the bulk has been observed. The continuous density-of-states in the valence or conduction band gives rise to energetically broad distributions of target *K*-shell Auger electrons. Consequently, no sharp atomic lines are observed. To our knowledge, up to now no indications for ion induced sputtering of hollow atoms or ions with *K*-shell vacancies has been observed. On the contrary, it is known that by far the largest fraction of sputtered material leaves the surface in the neutral state [22]. Although for keV projectiles the sputter yields generally increase with the charge state of the incidence ion (up to the order 100–1000 atoms/incident ion [23–25]), even for impact of Au^{69+} on uranium oxide [26] and Th^{70+} on GaAs [25], the ionic fractions of these yields are below 1% and 0.1%, respectively.

In the following we present experimental results that strongly indicate the presence of hollow atom/ion sputtering in grazing collisions of hydrogenlike ions with carbon surfaces.

II. EXPERIMENT

In our paper we used hydrogenlike ions C^{5+}, N^{6+}, and O^{7+} extracted from the *KVI* electron cyclotron resonance ion source operated at a potential of 8 kV. The ions were decelerated by floating the complete setup onto source potential and biasing it with a voltage V_{bias} such, that the projectile energy equals $q \times V_{\mathrm{bias}}$ (q being the projectile charge state). Target currents were of the order of 100 nA. During the measurements the base pressure was about 4×10^{-10} mbar. The HOPG(0001) target was prepared *ex situ* by means of the standard ''scotch tape'' method. The final preparation was done by series of grazing incidence (5°–10°) 800 eV Ar sputtering-annealing cycles. C_{60} monolayers on Au(111) were produced following the recipe suggested by Tjeng *et al.* [27]: A large amount of C_{60} is deposited at room temperature on the (thoroughly sputtered) Au(111). Desorption of bulk C_{60} starts at 180 °C, whereas the much stronger

*Electronic address: tschlat@kvi.nl; URL: kvip56.kvi.nl

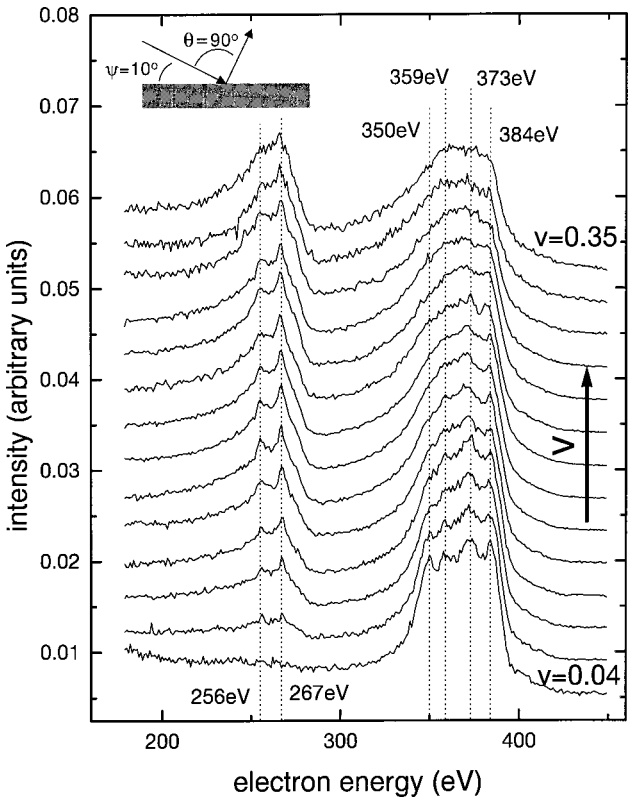

FIG. 1. *KLL* and *KVV* electron spectra from N^{6+} scattered off HOPG. The incidence and observation angles are 10° and 90°, respectively. The projectile velocity varies between 0.04 and 0.35 a.u. in steps of 0.025 a.u.

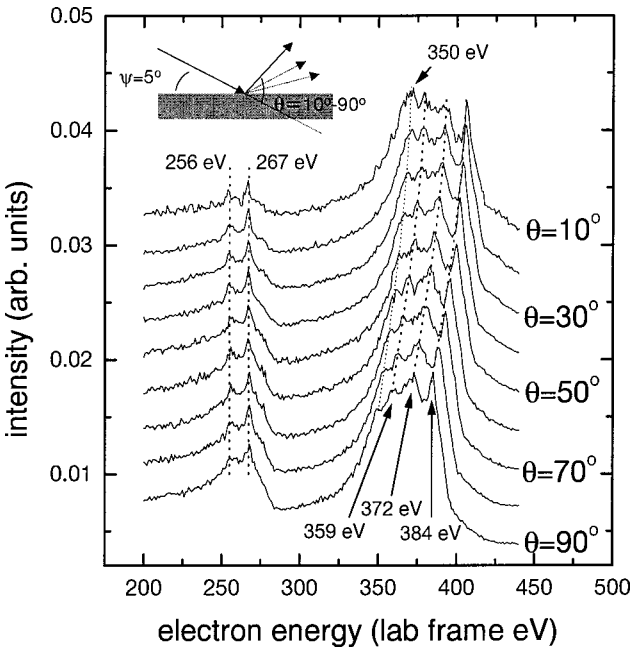

FIG. 2. *KLL* and *KVV* electron spectra from N^{6+} scattered off HOPG at $v=0.15$ a.u. The incidence angle is 5°. The observation angle θ varies between 10° and 90°.

C_{60}-Au(111) bond only breaks at temperatures higher than 360 °C. Thus, a monolayer covering the complete Au(111) surface can be formed by heating the sample to 300° for a few minutes. Removal of the fullerene layer is accomplished by heating up to 400 °C.

Electron spectra arising from the ion-surface interaction were measured using a 180° spherical electrostatic analyzer. The detector can be rotated in order to vary the electron observation angle θ measured with respect to the incident beam over a wide range from 0° to 140°. The energy resolution is $\Delta E/E=0.5\%$ full width at half-maximum with an acceptance of $11.2\times10^{-8}E(\mathrm{sr\,eV})$, E being the energy of the detected electrons. A detailed description of the setup can be found in Ref. [28].

III. RESULTS

A set of high-resolution Auger spectra from N^{6+} collisions with HOPG is displayed in Fig. 1. The detection angle θ was 90° with respect to the beam and the projectiles were scattered under a glancing angle $\psi=10°$. The measurements were done at projectile velocities between $v=0.04$ a.u. and $v=0.34$ a.u. corresponding to kinetic energies ranging from 0.44 to 42 keV. An offset proportional to the velocity has been added to the spectra. All spectra have been normalized to an equal integral over the projectile *KLL* peak between 320 and 450 eV. At the lowest velocities, the broad nitrogen *KLL* peak shows discrete structures that can be attributed to emission from projectiles with a filled L shell ($E=384$ eV), projectiles with a highly inverted population, i.e., only two electrons in the L shell ($E=350$ eV), or from projectiles with L-shell fillings in between these extreme cases. The relative intensity of the discrete peaks changes with the projectile velocity v.

However, the most striking feature of the spectra is the Auger peak between 200 and 280 eV, which we attribute to target Auger emission from C atoms. The ratio between target and projectile Auger electrons in Fig. 1 changes dramatically with increasing v: For $v=0.04$ a.u. no target Auger emission is observed, whereas at $v=0.35$ a.u. comparable numbers of target and projectile Auger electrons are found. A closer look at the target Auger peaks at intermediate velocities reveals discrete peaks on top of a broad background. This finding is very remarkable, since the target Auger electrons are expected to originate from bulk graphite. The Auger line shape should then be given by a self-convolution of the target density-of-states (DOS). Even though the graphite DOS has three broad maxima due to the π_p, σ_p, and σ_s bands, in the resulting *KVV* (V denoting the valence band) Auger peak, all structures are washed out [29] (see also Fig. 5).

To pinpoint the origin of the C-Auger electrons we exploit the Doppler shift of electrons emitted from the projectile when θ differs from the perpendicular observation angle used in Fig. 1. In Fig. 2 Auger spectra for constant velocity $v=0.15$ a.u. measured at different observation angles are displayed. The incidence angle ψ is always 5°. An offset proportional to the observation angle θ has been added to the spectra. As in Fig. 1, projectile as well as target Auger peaks are observed. As expected, the complete *NKLL* structure

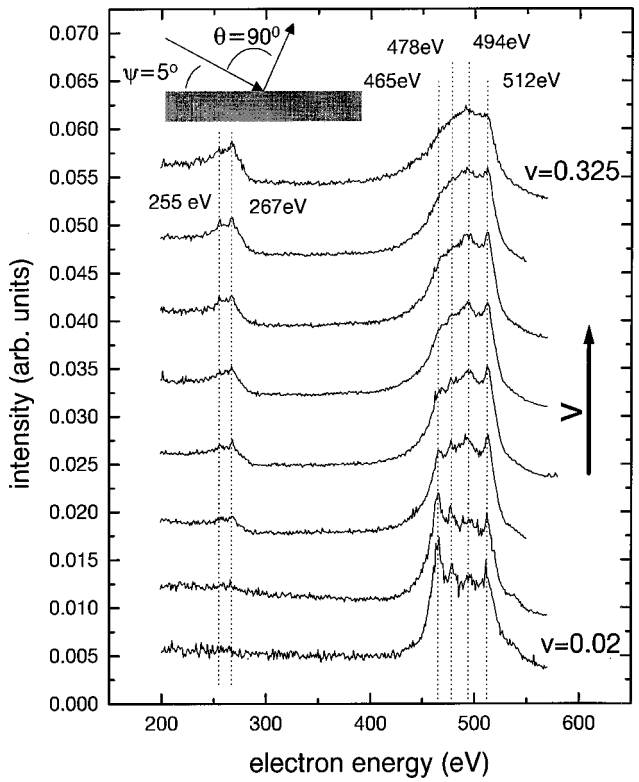

FIG. 3. *KLL* and *KVV* electron spectra from O^{7+} scattered off HOPG. The incidence and observation angles are 5° and 90°, respectively. The projectile velocity varies between 0.02 and 0.325 a.u. in sets of 0.04 a.u.

Doppler shifts to higher energies when θ is decreasing. The calculated energetic positions for the peaks at 359, 372, and 384 eV are indicated by the dotted lines. It is obvious, that the 384 eV peak is becoming relatively more intense for small θ, partly because the corresponding electrons can be emitted on the outgoing part of the trajectory and still be detected. Furthermore, the (above-surface emission) peak at 350 eV becomes more prominent with decreasing θ. This is due to the fact, that the other contributions partly originate from below surface emission processes. For very small observation angles, the corresponding electrons suffer a strong attenuation due to the increasing pathlength through the HOPG bulk.

The target Auger distribution between 200 and 280 eV shows no Doppler shift at all. In particular, the discrete structures at 256 and 267 eV are unchanged upon projectile velocity variation. With decreasing observation angle, their relative intensity with respect to the broad background increases strongly. This indicates, that the discrete peaks originate from the topmost layer or above, whereas the broad structure exhibits the typical angular distribution expected for *KVV* emission processes in bulk HOPG.

As outlined before, the *KVV* emission is probably initiated by *K*-shell vacancy transfer from the projectile to the target. It is therefore a logic test to investigate the interaction of different projectiles with the HOPG target. The results for O^{7+} projectiles are displayed in Fig. 3. The detection angle θ was 90° with respect to the beam and the projectiles were

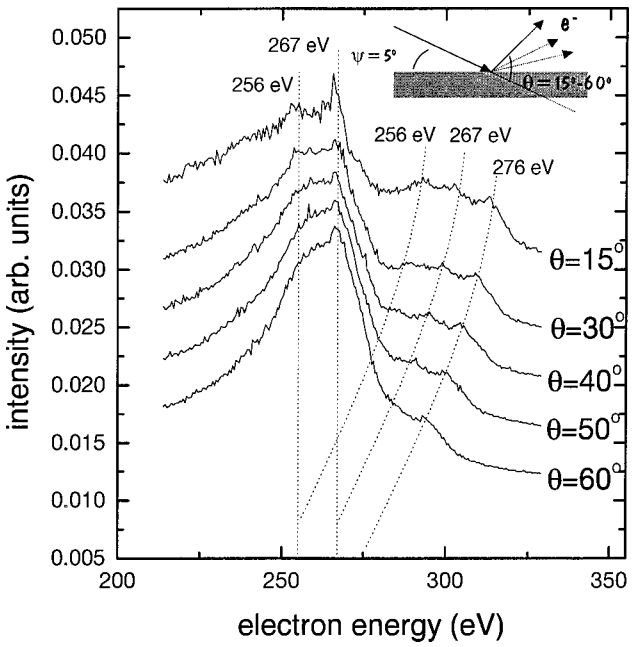

FIG. 4. *KLL* and *KVV* electron spectra from O^{5+} scattered off HOPG at $v=0.3$ a.u. The incidence angle is 5°. The observation angle θ varies between 15° and 60°.

scattered under $\psi=5°$ and the measurements were done at projectile velocities between $v=0.02$ a.u. and $v=0.325$ a.u., i.e., the experimental parameters are very similar to those for the N^{6+} case (Fig. 1). Again, the spectra consist of a structure due to projectile *KLL* Auger electrons (around 500 eV) as well as the target *K* Auger electrons between 200 and 280 eV. Obviously, relatively much less target Auger electrons are produced with O^{7+} as compared to N^{6+}. Also the discrete peaks superimposed on the broad *KVV* background are weaker.

On the other hand, the strongest effects can be expected for collision of C^{5+} with HOPG. This system is difficult to study, since projectile and target Auger electrons are expected at the same energies. However, we can avoid this problem by using fast projectiles and separate both contributions by exploiting the Doppler shift of the electrons emitted from the projectile.

Figure 4 shows results for $v=0.31$ a.u. C^{5+} impact on HOPG scattered under $\psi=5°$. The detection angle θ varies between 15° and 60°. The difference of the ratio between target-Auger peak and projectile-Auger peak when going from O^{7+} and N^{6+} projectiles to C^{5+} is dramatic. For large values of θ it is hard to separate projectile and target Auger distributions, but for $\theta=15°$ the two structures can be clearly distinguished. Even for this small detection angle, the integral over the target Auger distribution exceeds the one originating from the projectile. This is even more surprising since we know from Fig. 2, that at small angles the relative intensity of the target *KVV* Auger electrons originating from the bulk (broad structure) is strongly supressed. Furthermore, the projectile Auger distribution clearly shows a prominent peak at 276 eV originating from the $C\,1s2s^22p^3$ configuration. For target Auger emission following a vacancy transfer to the C *K* shell, this is the expected configuration. On the other

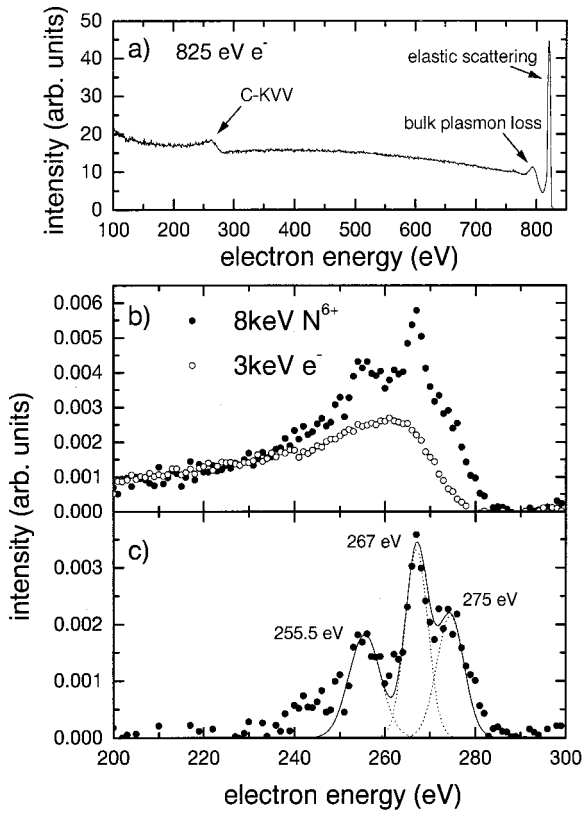

FIG. 5. (a) Raw electron spectrum from 825 eV electron impact on HOPG. (b) Background substracted C Auger peak from 3 keV electron and 8 keV N^{6+} impact on HOPG. For the electron impact measurements, the incidence angle ψ is 20° and the observation angle θ equals 70°. In (c) the difference spectrum of the data in (b) is displayed.

hand, it seems that the 276 eV peak is barely present in the target Auger spectra for C^{5+}, N^{6+}, and O^{7+} (see Figs. 1–4).

IV. DISCUSSION

As pointed out in the previous section, the target Auger electron spectra consist of discrete peaks superimposed on a broad background. To clarify the origin of both components, two different approaches are straightforward: (i) the Auger spectra can be compared to results obtained using another excitation mechanism, e.g., electrons; (ii) a different carbon allotrope can be used as a target, in order to provide a different electronic structure.

Figure 5(a) displays an electron spectrum obtained by impact of 825 eV electrons on HOPG. The elastic scattering peak can be found slightly below 825 eV. About 25 eV below the elastic peak a second maximum is observed, which can be attributed to electron energy loss due to excitation of a bulk plasmon. We are mainly interested in the weaker feature around 260 eV: The C *KVV* Auger electrons from the bulk HOPG are superimposed on a strong background of inelastically scattered electrons. The background substracted C *KVV* peak obtained from a 3 keV electron impact induced electron spectrum is shown in Fig. 5(b) (open symbols). It is compared to the background substracted C Auger peak from 8 keV N^{6+} scattered off HOPG. The difference spectrum of both distributions [Fig. 5(c)] should give an idea of the electron spectrum due to above surface target Auger emission. By and large it can be described by three peaks centered at about 255.5, 267, and 274.5 eV. The exact energetic position of the C Auger lines are compiled together with projectile C *KLL* Auger data from Ref. [6] in Table I. It is obvious that the energetically highest peak at 275 eV, which is due to *KLL* emission from a $1s2s^22p^3$, has not been observed in the C projectile *KLL*-Auger spectra of the earlier study on Si, W, and Ni. The appearance of the 275 eV peak here fits perfectly into the *K*-shell vacancy transfer picture: A *K*-shell electron is removed from a ground-state atom within the surface, and the resulting C atom with $1s2s^22p^3$ configuration is sputtered from the surface.

As mentioned earlier, the electrons emitted from bulk HOPG, i.e., the C *KVV* fraction, are suppressed for small observation angles θ. Figure 6 shows a zoom into the region of interest of the $\theta=20°$ spectrum from Fig. 2. The spectrum also mainly consists of three peaks centered at 255.5, 267, and 275 eV. The peak ratios and the background differ from Fig. 5(c) because of the persistence of a small fraction of *KVV* electrons originating from the bulk.

However, at about the same energies three C Auger peaks are also found in the (Doppler shifted) projectile C *KLL* spectra (Fig. 4). This similarity seems to indicate, that the discrete components of the target Auger distribution are due to the decay of hollow atoms above the surface moving at low velocity (without Doppler shift).

In that case, the discrete components should not depend

TABLE I. Energetic positions of carbon *KLL* peaks measured for C^{5+} impact on HOPG and other targets [Si(100), W, and Ni(110) taken from a compilation of Limburg *et al.* [6]] and calculated positions for different final configurations starting from an initial $1s2l^23l^3$ configuration [30] (○: not present, ●: unclear).

Conf.	Calc.	HOPG	Si(100)	W	Ni(110)
A $1s(2s^2\ ^1S)^2S$	248	●	248±2	250±2	245±2
B $1s(2s2p^3P)^2P$	256	255.5	256±2	●	●
C $1s(2s2p\ ^1P)^2P$	261	○	●	●	●
D $1s(2s2p^2\ ^3P)^2P$	262	○	●	●	●
E $1s(2s2p^2\ ^1D)^2D$	265	267	265±2	264±2	264±2
F $1s(2s2p^2\ ^1S)^2S$	271	○	○	○	○
G $1s2s^22p^3$	274	275	○	○	○

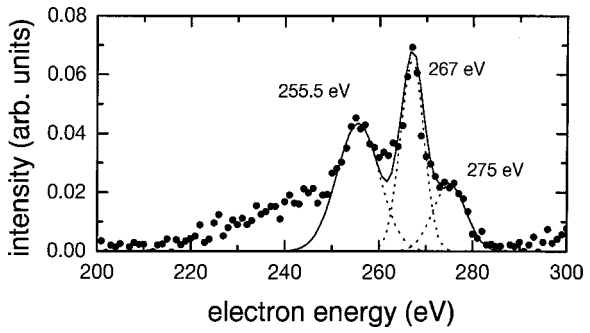

FIG. 6. C Auger distribution of the $\theta = 20°$ spectrum from Fig. 2.

on the target electronic structure, i.e., the same results are expected for interaction of hydrogenlike ions with different carbon allotropes. In Fig. 7 target Auger spectra for $v = 0.13$ a.u. N^{6+} impact on HOPG and C_{60} covered Au(111) are shown. Obviously both spectra are basically identical. In particular, the locations of the discrete peaks are the same.

Due to the strong velocity dependence of the C *K*-Auger yield apparent from Figs. 1 and 2 a C *K*-shell ionization due to *KLL* electrons from the projectile can be ruled out as a dominant process: for such secondary processes, only a weak velocity dependence is expected [21].

Thus, for collisions of hydrogenlike ions with carbon targets, a certain class of trajectories exists, in which a *K*-shell vacancy is transferred from the projectile to a surface atom that is sputtered from the surface—probably in the same collision process. Such a process is only possible under three conditions: (A) The interaction time between projectiles and surface is short in order to sustain *K*-shell vacancies until the collision occurs. (B) The collision energy has to be high enough to allow direct sputtering of surface atoms. (C) A vacancy transfer has to be possible.

A. Projectile-surface interaction times

The first condition is necessary for the occurence of target Auger electron emission in general and deserves a thorough discussion. According to the classical over-the-barrier model a current of electrons starts to flow from the solid to the

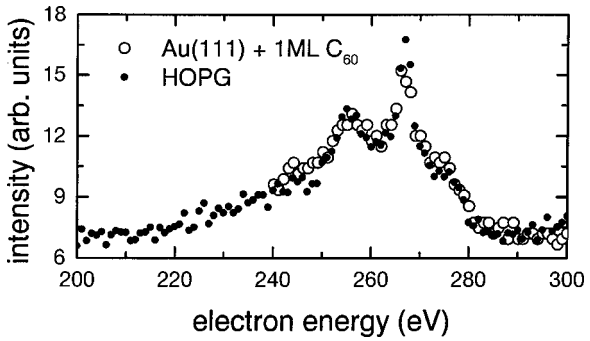

FIG. 7. Target Auger spectra from N^{6+} scattered off HOPG and a monolayer C_{60} film on Au(111) at $v = 0.13$ a.u. The incidence angle ψ is 5° and the detection angle θ is 90° and 50° for the HOPG and the C_{60} target, respectively.

projectile as soon as the saddle point of their joint potential is energetically lower than the surface work function [18]. Capture sets in at a critical distance $R_c \approx (1/2W)\sqrt{8q+2}$ with the work function W ($W_{\mathrm{HOPG}} = 4.7$ eV [31]) and the projectile charge state q. For $q = 5,6,7$ (the hydrogenlike projectiles C^{5+}, N^{6+}, and O^{7+}) the respective distances are $R_c = 18.8$, 20.5, and 22.0 a.u.

Below a distance R_c the projectile is neutralized by electron capture from the surface valence band into Rydberg states. Subsequent Auger transitions then fill the *L* shell. Thomaschewski *et al.* [32] found that the key parameter for the above-surface *L*-shell filling of N^{6+} in front of an Au(111) surface is the perpendicular component of the velocity. At closer distances, two-center *LVV* processes take over, in which both involved electrons stem from the surface valence band. For this class of trajectories it has been shown by Limburg *et al.* [33] that the neutralization and subsequent deexcitation of hydrogenlike ions in front of various surfaces strongly depends on the frequency of close collisions between projectile and surface atoms, i.e., on the parallel projectile velocity. The transition rates for the *L*-Auger processes themselves are velocity independent and depend weakly on the number of *L*-shell electrons already present. For an *LVV*-Auger process into the *L*-shell of an N ion for instance the transition rate is $\approx 1 \times 10^{15}\,\mathrm{s}^{-1}$ for electron densities comparable to the graphite case ($r_s = 1.5$ a.u.) [34]. This is only one order of magnitude faster than typical *KLL*-Auger transition times that lie in the 10^{14}–$10^{13}\,\mathrm{s}^{-1}$ range and therefore *KLL* decay sets in as soon as two electrons are present in the *L* shell, at a time when the projectile is still above the surface. The corresponding peak in the electron spectra for N^{6+} impact is due to a $1s2s^2\ ^2S$ configuration and can be found at 350 eV (Fig. 1). The fact that this peak is only present for very low-collision velocities already indicates, that a second velocity dependent *L*-shell filling process is active. Most probably for closer distances, the *L* shell is filled quasiresonantly in a Landau-Zener type electron transfer during close binary collisions [4]. The frequency of such collisions scales with the projectile velocity v. With increasing projectile velocity, the fast direct filling of the projectile *L* shell becomes more important and *KLL* emission from more completely filled *L*-shell systems sets in. From Fig. 1 it is obvious, that for N^{6+} scattering from HOPG, even for low v emission from the filled *L* shell, takes place and the low-energy peak never becomes as prominent as observed in collisions with metal and semiconductor targets [6]. Above $v = 0.1$ a.u. it even completely vanishes. From this we conclude, that projectile *KLL*-Auger emission at higher v takes place at or below the surface.

Therefore for $v > 0.1$ a.u. condition (A) is clearly fulfilled. At lower v, only a fraction of *K*-shell vacancies survives, giving rise to a drop in target Auger emission. In conclusion, the presence of the low-energy projectile *KLL* peak might serve as a fingerprint for a situation in which no or little target Auger emission is expected.

B. Surface penetration and sputtering

To answer the second question, namely, from which velocity on the projectiles penetrate the surface and/or sputter

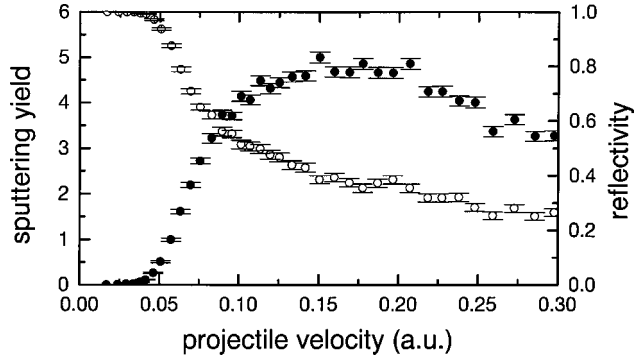

FIG. 8. Sputtering yield (solid circles) and reflectivity (open circles) of a HOPG surface upon N impact as a function of the projectile velocity v. The geometry is chosen as in Fig. 1.

C atoms, we performed simulations based on the binary collision approximation using the MARLOWE code and time-ordered cascades [35,36]. Sputter yields as well as the surface reflectivity for scattering of N from HOPG ($\psi=10°, v=0.02-0.3$ a.u.) can be found in Fig. 8.

A strong threshold effect is visible for both quantities: At about 0.05 a.u., the projectiles start to penetrate the surface and the sputtering yield increases dramatically. To compare this directly to the experimental data, we extracted the target-*K*-Auger to projectile-*KLL* ratios as a function of v for N^{6+} and O^{7+} projectiles (Fig. 9).

Both data sets show an increase with v. In the case of N^{6+} the ratio rises strongly around $v=0.05$ a.u., as expected from the simulation as well as from the experimentally observed survival probability of the *K*-shell vacancy, i.e., the absence of a high-energy peak in the projectile *KLL*-Auger distribution. From this data it is unclear, which one is the limiting factor for target Auger emission.

The O^{7+} data in Fig. 9 have been measured with an incidence angle $\psi=5°$, i.e., in a less destructive mode. The results of the simulation of sputtering yield and reflectivity for O impinging on HOPG can be found in Fig. 10. Sputtering and penetration set in at $v=0.1$ a.u., which is much higher than in the N^{6+} case. However, in the *K*-Auger ratios from

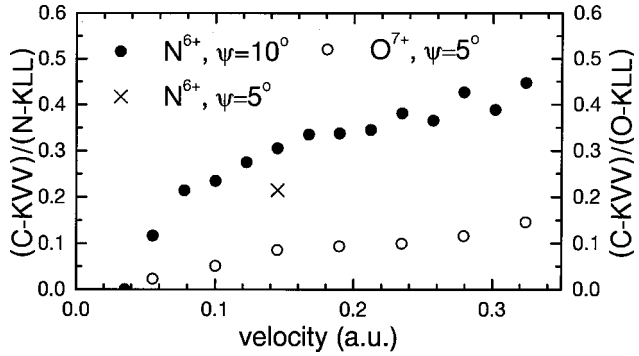

FIG. 9. Target *KVV* to projectile-*KLL* ratios versus v for N^{6+} (left axis, full circles, $\psi=10°$) and O^{7+} (right axis, open circles, $\psi=5°$) scattered off HOPG. The data are taken from Figs. 1 and 3 and have been background substracted. The additional data point (x) at $v=0.15$ a.u. belongs to the N^{6+} but has been measured under the same geometry as the O^{7+} ($\psi=5°$).

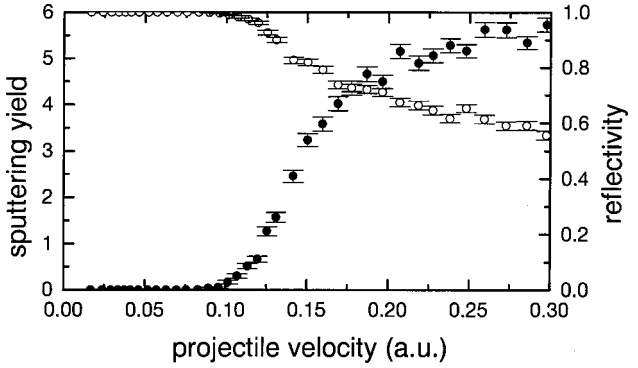

FIG. 10. Sputtering yield (solid circles) and reflectivity (open circles) of a HOPG surface upon oxygen impact ($\psi=5°$) as a function of the projectile velocity v. The geometry is chosen as in Fig. 3.

Fig. 9, no threshold is visible at all. In particular target Auger emission is observed well below the $v=0.1$ a.u. threshold. On the other hand, the appearance of the low-energy peak in the projectile *KLL*-Auger distribution ($E=465$ eV) in Fig. 3 coincides with the vanishing of the target Auger peak thus indicating that the survival of the *K*-shell vacancy is the limiting factor for target Auger emission. Apparently even for velocities lower than the threshold from Fig. 10, imperfections of the surface may still give rise to some surface penetration and sputtering. However, the fact that the sputtering is less effective than for the N^{6+} case manifests itself in the relatively weak discrete peaks within the target Auger distribution (which we assign to *KLL*-Auger emission from sputtered carbon).

C. *K*-shell vacancy transfer

From Fig. 9 it is also obvious, that the relative target Auger yield is significantly higher for N^{6+} than for O^{7+}. Part of the reason is the larger ψ for the N^{6+} data, therefore Fig. 9 also contains an N^{6+} data point measured under the same scattering geometry as the O^{7+} data ($\psi=5°$). The relative values at $v=0.15$ a.u. are 0.215 (N^{6+}) and 0.085 (O^{7+}), i.e., at this velocity with oxygen projectiles 60% less target Auger electrons are observed.

The reason has to lie in the projectile dependence of the vacancy-exchange mechanism. In the past, a variety of inner-shell vacancy exchange mechanisms have been proposed and used succesfully. We applied the model of Schippers *et al.* [4] which assumes Landau-Zener-like vacancy exchange in close binary collisions. However, in Ref. [4] collisions of N^{6+}, O^{7+}, and Ne^{9+} ($v\approx 0.4$ a.u.) with Pt(110) were studied, where vacancy transfer between projectile *K*-shell and target *N* shells is dominating. The level crossings occur at internuclear distances between 0.5 and 1 a.u., which can easily be reached at such high velocities. In our paper the C *K* shell is involved and vacancy transfer from the projectile *K* shell or *L* shell takes place at even smaller internuclear distances. In particular, in the low-projectile velocity regime, these distances can hardly be reached and the resulting vacancy exchange probabilities are negligible. Only for the symmetric case of a C projectile at high v, considerable exchange prob-

ability from the projectile L shell to the target K shell is obtained. At $v=0.3$ a.u. on average 5 C atoms are sputtered by each projectile, i.e., several close collisions take place, each with a considerable vacancy exchange probability. This could lead to an increased vacancy transfer probability, which could explain the experimental results obtained with C^{5+} projectiles, but not the O^{7+} and N^{6+} case. The reason for the nonapplicability of the Landau-Zener approach from Ref. [4] might lie in the semi-metallic structure of the HOPG, which gives rise to a screening that differs from the metal case.

V. SUMMARY

The interaction of slow ($v<0.4$ a.u.) hydrogenlike ions with carbon surfaces leads to strong target K-Auger emissions. These Auger electrons partly originate from bulk or surface carbon (KVV-Auger electrons). A second fraction of the carbon K-Auger electrons exhibits distinct peaks, which can be identified as being due to atomic KLL transitions. We presented strong indications that these target KLL electrons are fingerprints of a yet undiscovered process, namely, sputtering of hollow atoms from the surface.

ACKNOWLEDGMENTS

The authors gratefully acknowledge financial support from the Stichting voor Fundamenteel Onderozoek der Materie (FOM) which is supported by the Nederlandse Organisatie voor Wetenschapelijk Onderzoek (NWO). A.N. acknowledges financial support from the NWO visitors program.

[1] A. Arnau *et al.*, Surf. Sci. Rep. **27**, 117 (1997).
[2] H. Khemliche, T. Schlathölter, R. Hoekstra, R. Morgenstern, and S. Schippers, Phys. Rev. Lett. **81**, 1219 (1998).
[3] F. W. Meyer, S. H. Overbury, C. C. Havener, P. A. Zeijlmans van Emmichoven, and D. M. Zehner, Phys. Rev. Lett. **67**, 723 (1991).
[4] S. Schippers, S. Hustedt, W. Heiland, R. Köhrbrück, J. Bleck-Neuhaus, J. Kemmler, D. Lecler, and N. Stolterfoht, Phys. Rev. A **46**, 4003 (1992).
[5] H. J. Andrä, A. Simionovici, T. Lamy, A. Brenac, and A. Pesnelle, Europhys. Lett. **23**, 361 (1993).
[6] J. Limburg, J. Das, S. Schippers, R. Hoekstra, and R. Morgenstern, Surf. Sci. **313**, 355 (1994).
[7] J. Limburg, J. Das, S. Schippers, R. Hoekstra, and R. Morgenstern, Phys. Rev. Lett. **73**, 786 (1994).
[8] J. Limburg, S. Schippers, R. Hoekstra, R. Morgenstern, H. Kurz, F. Aumayr, and H. Winter, Phys. Rev. Lett. **75**, 217 (1995).
[9] N. Stolterfoht, A. Arnau, M. Grether, R. Köhrbrück, A. Spieler, R. Page, A. Saal, J. Thomaschewski, and J. Bleck-Neuhaus, Phys. Rev. A **52**, 445 (1995).
[10] M. Schulz, C. Cocke, S. Hagmann, M. Stöckli, and H. Schmidt-Böcking, Phys. Rev. A **44**, 1653 (1991).
[11] B. d'Etat, J. Briand, G. Ban, L. de Billy, J. Desclaux, and P. Briand, Phys. Rev. A **48**, 1098 (1993).
[12] Y. Yamazaki, S. Ninomiya, F. Koike, H. Masuda, T. Azuma, K. Komaki, K. Kuroki, and M. Sekiguchi, J. Phys. Soc. Jpn. **65**, 1199 (1996).
[13] D. M. Zehner, S. H. Overbury, C. C. Havener, F. W. Meyer, and W. Heiland, Surf. Sci. **178**, 359 (1986).
[14] F. W. Meyer, C. C. Havener, K. J. Snowdon, S. H. Overbury, D. M. Zehner, and W. Heiland, Phys. Rev. A **35**, 3176 (1987).
[15] P. A. Zeijlmans van Emmichoven, C. C. Havener, and F. W. Meyer, Phys. Rev. A **43**, 1405 (1991).
[16] R. Köhrbrück, K. Sommer, J. Biersack, J. Bleck-Neuhaus, S. Schippers, P. Roncin, D. Lecler, F. Fremont, and N. Stolterfoht, Phys. Rev. A **45**, 4653 (1992).
[17] S. Winecki, C. Cocke, D. Fry, and M. Stöckli, Phys. Rev. A **53**, 4228 (1996).
[18] J. Burgdörfer, P. Lerner, and F. W. Meyer, Phys. Rev. A **44**, 5674 (1991).
[19] L. Hägg, C. O. Reinhold, and J. Burgdörfer, Phys. Rev. A **55**, 2097 (1997).
[20] J. J. Ducree, F. Casali, and U. Thumm, Phys. Rev. A **57**, 338 (1998).
[21] U. Lehnert, M. Stöckli, and C. Cocke, J. Phys. B **31**, 5117 (1998).
[22] A. Benninghoven, Surf. Sci. **299/300**, 246 (1994).
[23] S. T. deZwart, T. Fried, D. A. Boerma, R. Hoekstra, A. G. Drentje, and A. L. Boers, Surf. Sci. **177**, L939 (1986).
[24] M. Sporn, G. Libiseller, T. Neidhart, M. Schmid, F. Aumayr, H. Winter, and P. Varga, Phys. Rev. Lett. **79**, 945 (1997).
[25] T. Schenkel, A. V. Hamza, A. V. Barnes, D. H. Schneider, J. C. Banks, and B. L. Doyle, Phys. Rev. Lett. **81**, 2590 (1998).
[26] T. Schenkel, A. V. Barnes, A. V. Hamza, D. H. Schneider, J. C. Banks, and B. L. Doyle, Phys. Rev. Lett. **80**, 4325 (1998).
[27] L. Tjeng, R. Hesper, A. Hessels, A. Heeres, H. Jonkman, and G. Sawatzky, Solid State Commun. **103**, 31 (1997).
[28] S. T. deZwart, A. G. Drentje, A. L. Boers, and R. Morgenstern, Surf. Sci. **217**, 298 (1989).
[29] J. Houston, J. Rogers, R. Rye, F. Hutson, and D. Ramaker, Phys. Rev. B **34**, 1215 (1986).
[30] S. Schippers, J. Limburg, J. Das, R. Hoekstra, and R. Morgenstern, Phys. Rev. A **50**, 540 (1994).
[31] I. Schäfer, M. Schlüter, and M. Skibowski, Phys. Rev. B **35**, 7663 (1987).
[32] J. Thomaschewski, J. Bleck-Neuhaus, M. Grether, A. Spieler, and N. Stolterfoht, Phys. Rev. A **57**, 3665 (1998).
[33] J. Limburg, S. Schippers, I. Hughes, R. Hoekstra, R. Morgenstern, S. Hustedt, N. Hatke, and W. Heiland, Phys. Rev. A **51**, 3873 (1995).
[34] R. Díez Muiño, N. Stolterfoht, A. Arnau, A. Salin, and P. M. Echenique, Phys. Rev. Lett. **76**, 4636 (1996).
[35] M. T. Robinson, Phys. Rev. B **40**, 10 717 (1989).
[36] M. T. Robinson, Nucl. Instrum. Methods Phys. Res. B **48**, 408 (1990).